Fluid Phase Equilibria 349 (2013) 1–11

Contents lists available at SciVerse ScienceDirect

Fluid Phase Equilibria

journal homepage: www.elsevier.com/locate/fluid

Phase behavior of carbon dioxide + medroxyprogesterone acetate system at high pressures

L.F. Pinto[a], S.B. Rodriguez-Reartes[b], M.L. Corazza[c], V.F. Cabral[a], P.H.H. de Araújo[d], E.H. Madureira[e], M.S. Zabaloy[b], L. Cardozo-Filho[a,*]

[a] Department of Chemical Engineering, State University of Maringá, 87020-900 Maringá, PR, Brazil
[b] Departamento de Ingeniería Química, Universidad Nacional del Sur, PLAPIQUI – CONICET, CC 717, 8000 Bahía Blanca, Argentina
[c] Department of Chemical Engineering, Federal University of Paraná, 81531-990 Curitiba, PR, Brazil
[d] Department of Chemical and Food Engineering, Federal University of Santa Catarina, 88040-900 Florianópolis, SC, Brazil
[e] Department of Animal Reproduction, Faculty of Veterinary Medicine, University of São Paulo, Pirassununga, SP, Brazil

ARTICLE INFO

Article history:
Received 6 February 2013
Received in revised form 14 March 2013
Accepted 20 March 2013
Available online 4 April 2013

Keywords:
Phase equilibrium
Medroxyprogesterone acetate
CO_2
Supercritical
Equation of state

ABSTRACT

In this study the phase equilibrium behavior of the binary system CO_2 (1) + medroxyprogesterone acetate (2) was determined. The static synthetic method, using a variable-volume view cell, was employed to obtain the experimental data in the temperature range of 303.15–343.15 K and pressures up to about 22 MPa. The mole fraction of medroxyprogesterone acetate varied in the range from 4×10^{-5} to 9×10^{-5}. For this system (fluid + solid) and (fluid + fluid + solid) transitions were observed. The phase equilibrium data obtained in this work were modeled using the Peng–Robinson equation of state for describing fluid mixtures, and an expression for the fugacity of pure solid medroxyprogesterone acetate (MPgAc) for representing the solid phase. The thermodynamic model was able to satisfactorily describe the phase behavior of the system investigated.

1. Introduction

Various hormonal treatments are designed to synchronize the phases of the reproductive cycle of animals, which includes the estrus, i.e., the time when the lining of the uterus is thickest and the sex urge is at its height. In particular, the medroxyprogesterone acetate (MPgAc) has a clear importance in estrus induction protocols for cows, in post partum period, in the context of fixed-time artificial insemination (TAI) [1–4].

Medroxyprogesterone acetate (MPgAc) (pregn-4-ene-3, 20-dione, 17-hydroxy-6α-methyl-, acetate) is a synthetic derivative of progesterone (Fig. 1) [5]. Its contraceptive effect mainly results from the inhibition of ovulation [6]. MPgAc has several pharmacological actions on the endocrine system [6,7].

MPgAc is presented in the form of a white crystalline powder, odorless, stable in air, insoluble in water, but very soluble in chloroform, acetone, acetonitrile, dioxane and partially soluble in ethanol [8,9].

Recent investigations have shown that the knowledge of the phase behavior of steroids in supercritical fluids, such as CO_2, is an important step in the development of techniques for encapsulation and release of active nanoparticles with applications in pharmaceutical, cosmetic and veterinary industries [10–16].

However, the drug + biopolymer + pressurized fluid systems involve mixtures of highly asymmetric compounds, and thus the determination of the phase envelopes is complex, both experimentally and theoretically [17–20].

Alessi et al. [11] investigated the phase behavior of CO_2 + MPgAc in a pressure range from 11 to 22 MPa at temperatures of 313 K and 333 K. Asghari-Khiavi et al. [12] determined the solubility of MPgAc in CO_2 within a pressure range from 12.2 to 35.5 MPa and at temperatures from 308 to 348 K using a static method. The solubilities measured by Asghari-Khiavi et al. [12] are lower at all pressures than those measured by Alessi et al. [11]. In the work by Asghari-Khiavi et al. [12] samples of supercritical CO_2 saturated with MPgAc where withdrawn from an extraction vessel and analyzed with the help of a spectrophotometer. On the other hand, Alessi et al. [11] used a dynamic method where a stream of saturated CO_2 was flashed so that the CO_2 and MPgAc became completely separated. The amount of precipitated MPgAc was quantified by weighing the drug, and the amount of CO_2 determined using a wet gas meter [11].

* Corresponding author. Tel.: +55 44 30114749; fax: +55 44 30114793.
E-mail addresses: cardozo@deq.uem.br, lucio.cardozo@gmail.com (L. Cardozo-Filho).

0378-3812/$ – see front matter © 2013 Elsevier B.V. All rights reserved.
http://dx.doi.org/10.1016/j.fluid.2013.03.019

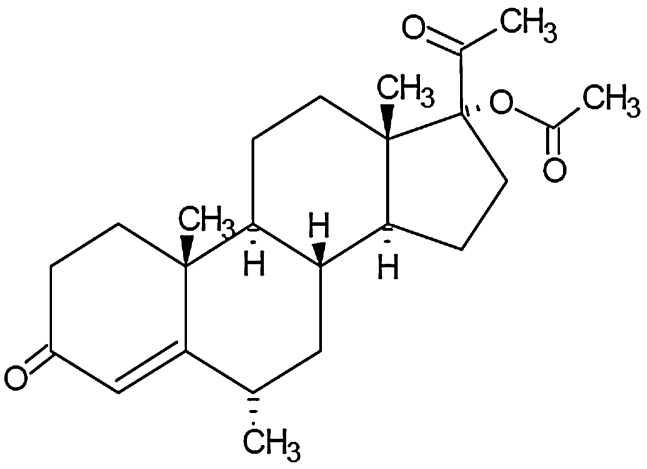

Fig. 1. Molecular structure of medroxyprogesterone acetate (MPgAc).

Both methods [11,12] are analytical, i.e., they require to measure the composition of the fluid mixture withdrawn either from a continuous extractor [11] or from a batch extractor [12]. Such analysis is involved because the mixture is asymmetric, i.e., made of components whose states differ significantly at ambient conditions (solid versus gas). In view of the disagreement between the solubility data of Refs. [11,12], it would be desirable to have available experimental phase equilibrium data for CO_2 + MPgAc obtained through an experimental technique alternative to those used by Alessi et al. [11] and Asghari-Khiavi et al. [12].

One such independent technique is the synthetic method, where the overall system composition is imposed (and known with high accuracy), and hence no portions of the fluid mixture need to be removed from the equilibrium cell to experimentally find the relationship among phase composition, temperature and pressure. For analytical methods, such as those of references [11] and [12], the measured solubility, i.e., the composition of the fluid phase at equilibrium with the solid phase, is expected to have a larger uncertainty in the low solubility range. This problem is minimized in the synthetic method, because the amount of solute loaded into the equilibrium cell is known with high accuracy. In this context, the main purpose of this work was to obtain, using the synthetic method, new solid–fluid equilibrium data for the system CO_2 + MPgAc, in the solubility range where analytical methods are less reliable (i.e., in the low solubility range), and to compare the new data with the data from Refs. [11,12].

With regard to the modeling of the solid–fluid equilibria of asymmetric systems, it is often found in the literature that the calculations are limited to the ranges of conditions of the experimental data (see, e.g., Fig. 2 in Ref. [12] and Fig. 5 in Ref. [11]). However, calculations extended to wider ranges of conditions, considering phase equilibria of different kinds (solid–fluid, fluid–fluid) and covering both, phase envelopes and heterogeneous regions, are convenient to gain a deeper insight on the possible behavior of the system under study. This is basically the approach used, for instance, by Giufrida et al. [21]. Another aim of the present work is therefore to apply such approach to the system CO_2 + MPgAc, not only for describing the new experimental data, but also to extend our comprehension of its phase behavior beyond the understanding that could be achieved on the grounds of solely the raw experimental data correlated only within the ranges of conditions of the experiments. The system CO_2 + MPgAc has a very complex phase behavior, as expected from its high size and polarity asymmetry. The correct modeling of this system is, therefore, a scientific challenge.

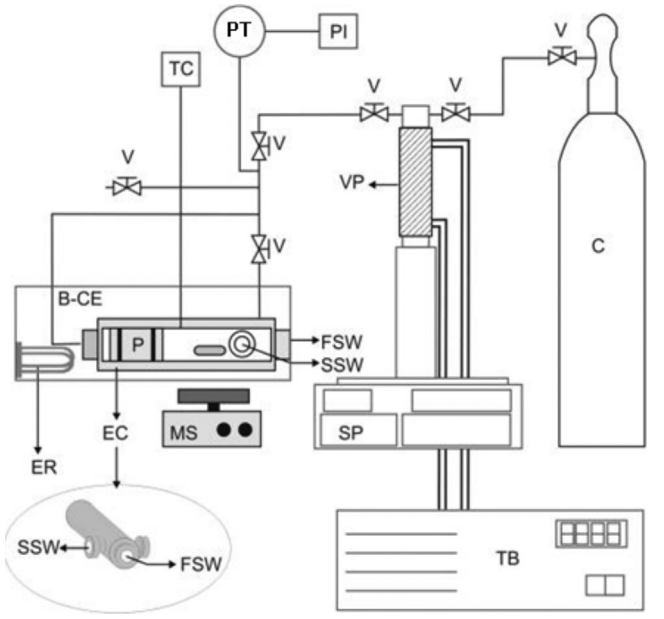

Fig. 2. Experimental setup. TB, thermostatic bath; SP, syringe pump; EC, equilibrium cell; MS, magnetic stirrer; TC, sensor of the temperature controller; B-EC, equilibrium cell thermostatic bath; ER, electrical resistance; PT, pressure transducer; PI, pressure indicator; P, movable piston; SSW, side sapphire window; FSW, front sapphire window; V, needle type valve; C, carbon dioxide cylinder; VP, vessel of the pump.

Alessi et al. [11] used an empirical form [their Eq. (1)] to correlate the drug solubility with the density of the pure supercritical fluid. Those are the only variables available to such correlation, which means that a variety of situations of interest, e.g., the conditions for solid–fluid–fluid equilibrium, cannot be computed. Alessi et al. [11] also used a modeling approach where the reference state is the sublimation point of the heavy component (the drug) at the system temperature, and the fluid phase is described by an equation of state. Such approach is applicable as long as the temperature is less than the triple point temperature of the (pure) heavy component. On the other hand, Asghari-Khiavi et al. [12] used a correlation that connects the pressure, the temperature, the solubility of the drug and the density of the pure supercritical solvent. Such correlation is not valid for low pressures [12]. In the present work, we have used an expression for the fugacity of pure solid MPgAc that is applicable, at least from the qualitatively point of view, at any temperature and pressure. To describe the fluid state, we have used the Peng–Robinson equation of state. Due to the high level of non-linearity of the phase equilibrium behavior of asymmetric systems, the required computations are best performed, as done in this work, with the help of numerical continuation methods.

2. Experimental

2.1. Materials

The carbon dioxide used here was purchased to White Martins and had a minimum mass fraction purity higher than 0.999. MPgAc (pregn-4-ene-3,20-dione, 17-hydroxy-6α-methyl-, acetate) was obtained from Sigma–Aldrich with minimum purity of 97%. The heat of fusion (ΔH_{2f}) and melting point temperature (T_m) of the MPgAc were measured in this work using Differential Scanning Calorimetry (DSC-50, Shimadzu), resulting in the values ΔH_{2f} = 88.76 J/g and T_m = 481 K. A Shimadzu UV spectrophotometer was used to obtain the wavelength of maximum absorption (λ) for MPgAc, using methanol as solvent. The resulting value was λ = 241 nm. Table 1 presents a comparison between the properties

Table 1
Physical properties of the medroxyprogesterone acetate.

Formula	MW (g/mol)	T_m (K)	Heat of fusion (J/g)	λ (nm)[a]
$C_{24}H_{34}O_4$	387	481[b]	88.76[b]	241[b]
		481[c]	–	240[c]

[a] Solvent: methanol.
[b] This work.
[c] Asghari-Khiavi et al. [12].

of MPgAc mesaured in this work (T_m and λ) and those obtained by Asghari-Khiavi et al. [12]. Clearly, the agreement is excellent. The information here obtained through DSC and spectrophotometry are indicative of the good level of purity of the MPgAc used in this work. All materials were used without further purification.

2.2. Phase equilibrium apparatus and experimental procedure

Phase equilibrium experiments were carried out employing a static synthetic method. Fig. 2 shows a schematic diagram of the experimental apparatus used here to obtain high-pressure phase transition data. The core of the equipment is a high pressure variable-volume view cell. The experimental apparatus and procedure have been previously used in a variety of studies made by our group [10,21–26].

Briefly, the experimental setup consists of a variable-volume view cell with two sapphire windows for visual observation, an absolute pressure transducer (Smar, model LD 301), with an accuracy of ±0.01 MPa, a portable programmer (Smar, model HT 201) for the pressure data acquisition, and a syringe pump (ISCO, model 260D).

The equilibrium cell contains a movable piston that permits the pressure control inside the cell. The cell is equipped with a water bath and PID controller (DIGI MEC mark, SHM 112 model).

The pressure transducer was calibrated against a digital multimeter HP-34401A model. The temperature controller was connected to a thermocouple (T type, accuracy ±1.0 K), which was in direct contact with the fluid mixture inside the equilibrium cell. The thermocouple was calibrated using a primary thermometer (Incoterm, 47342 model) at four fixed temperatures ranging from 273 to 373 K, providing a temperature control within 1.0 K. Fig. 2 shows the experimental apparatus used here to obtain high-pressure phase transition data.

Phase transitions were achieved by manipulating the pressure while keeping the temperature constant. Initially, the cell and all lines were flushed out with low-pressure CO_2 to remove residual air. An amount of MPgAc was weighed on a high accuracy scale (Ohaus Analytical Standard, uncertainty: 0.0001 g) and loaded into the cell. The amount of MPgAc was established according to the desired global composition. The syringe pump is maintained at fixed temperature and pressure. Under these constant conditions, the CO_2 was withdrawn from the syringe pump, and pumped into the cell, to reach the pre-established global composition. At the temperature and pressure of the syringe pump, the density of CO_2 was computed. This was necessary for the further calculation of the overall composition of the mixture loaded into the equilibrium cell.

Then, the cell content was kept at continuous agitation with a magnetic stirrer and a Teflon-coated stirring bar. After reaching the desired temperature, the cell pressure was increased by applying pressure on the back of the piston with the syringe pump, using CO_2 as an auxiliary fluid, until the system reached a single phase state. At this point, the system was allowed to stabilize for at least 30 min. This stabilization time was considered suitable after having performed a set of exploratory tests carried out for a range of stabilization times. For the systems studied in this work, the measured phase equilibrium was found to be insensitive to the stabilization time for stabilization times equal or greater than 30 min.

To promote a phase transition, the cell pressure was decreased slowly (typically at a rate of 0.1–0.3 MPa/min) until the incipient formation of another phase was observed through the sapphire window (static synthetic method).

The pressure was then recorded. The previous procedure was repeated at least three times, for each temperature and global composition, leading to experimental standard deviations in the order of 0.01–0.06 MPa. After completion of the measurement at a given temperature, the cell temperature was set at a new value and the experimental procedure was repeated.

On the basis of the uncertainties estimated for the masses of CO_2 and MPgAc introduced into the cell, it was possible to estimate, through propagation of error analysis, that the uncertainties in the here reported carbon dioxide and MPgAc mole fraction values were never greater than 10^{-4}% and 1.9%, respectively. These uncertainty levels were estimated using the procedure of Rodriguez-Reartes et al. [27]. In such work, the authors carried out their experiments using an experimental apparatus similar to the one used here.

3. Modeling of the phase behavior of the CO_2 + MPgAc system

In this work we modeled, according to Appendix A, the phase behavior of the binary system carbon dioxide (CO_2) + medroxiprogesterone acetate (MPgAc). We used the Peng–Robinson equation of state (PR-EOS) [28], with classical combining and mixing rules, for calculating component fugacities and phase densities in fluid state for pure compounds and mixtures. For solid–fluid and solid–fluid–fluid equilibrium calculations, we assumed that the solid phase is pure MPgAc, since the system CO_2 + MPgAc is highly asymmetric. The fugacity of the pure heavy component (MPgAc) in solid state at system temperature (T) and pressure (P), is given in this work by Eq. (1′) of Appendix A.

The set of equations for phase equilibrium calculations arises from imposing the classical necessary conditions: equal temperature, equal pressure, and equal component fugacities in all phases. With regard to the calculation algorithms, we used numerical continuation methods (NCMs) for all phase equilibrium computations [29–31] where a line is generated. As a "line" we mean, e.g., a solid–fluid equilibrium segment of an isopleth phase envelope. Each point of a phase equlibrium line corresponds to a non-linear system of equations. After a converged point has been obtained, the initialization of the next point of the line is performed by using a local linear representation of the line. This is done with the help of the sensitivity vector, whose elements are the derivatives of all variables with respect to the variable considered to be the independent one. In other words, this vector quantifies the sensitivity of the solution of the system of equations with respect to the value specified for the independent variable. Once a converged point is available, the sensitivity vector is easily computed by solving a linear system of equations. The expression for such system of equations is straightforwardly derived by applying the method of implicit differentiation to the equilibrium non-linear system of equations. Both, the identification of the optimum variable to be specified for obtaining the next point on the line, and its initialization, are carried out with the help of the sensitivity vector. NCMs are able to track phase equilibrium lines of varying shapes without failing to converge in the vicinity of turning points (local minima or maxima) or of self-intersection points. When using NCMs we have scaled the variables logarithmically. A more detailed description is available in Refs. [29–31].

We present, in Section 4.2, among other results, calculated isopleths which are characterized by segments corresponding to

fluid–fluid (FF) and solid–fluid (SF) equilibrium transitions (phase envelope of the isopleth), and by relevant solid–fluid–fluid (SFF) equilibrium segments (heterogeneous region of the isopleth).

3.1. Parameterization

For CO_2 we obtained the pure compound critical properties and acentric factor from the DIPPR database (see Table 3) [32]. For MPgAc, we estimated such information through the Constantinou and Gani group contribution method [33]. The obtained values are reported in Table 3 together with the calculated boiling temperature and critical volume for MPgAc. Table 1 reports the values for other MPgAc physical properties that we obtained experimentally in this work. For modeling purposes we have taken the MPgAc triple point temperature as equal to the experimental melting temperature (T_m) reported in Table 1.

To the best of our knowledge, there are no experimental data available for the pressure as a function of temperature for pure MPgAc under solid–liquid equilibrium conditions. Under such circumstances, the model used here has six parameters whose values need to be set, i.e., the binary interaction parameters k_{12} and l_{12} (of the Peng and Robinson equation of state), and the four parameters in Eq. (1′) of Appendix A, i.e., Δv^{S-L}, C_1, C_2 and C_3. Notice that these last four parameters are pure MPgAc parameters, while k_{12} and l_{12} are parameters characteristic of the binary system CO_2 + MPgAc. The values for the parameters k_{12} and l_{12} and for parameter Δv^{S-L} in Eq. (1′) of Appendix A (see Tables 4 and 5, respectively) were obtained by reproducing some selected experimental solid–fluid (SF) equilibrium data reported in Table 2 (see footnotes in Table 2). During the optimization, the C_i constants of Eq. (1′) of Appendix A were restricted as follows: $C_1 = -150$ MPa, $C_2 = 0$ MPa and $C_3 = 0$ MPa (see Table 5). This gives a calculated pure MPgAc liquid–solid equilibrium curve (not shown in this article) that has a positive slope; similar to the calculated slope for progesterone in a previous study [29].

More specifically, we have simultaneously adjusted the parameters (k_{12}, l_{12} and Δv^{S-L}) by minimizing the following objective function (*OF*):

$$OF = \sum_{NP} \left(1 - \frac{\hat{f}_2(T_{exp},\ P_{exp},\ x_{2,exp})}{f_2^S(T_{exp}, P_{exp})} \right)^2 \quad (1)$$

where T_{exp}, P_{exp}, $x_{2,exp}$ are respectively the experimental temperature, pressure and mole fraction of the heavy component in the fluid phase, for a binary solid–fluid equilibrium point with a solid phase made of the pure heavy component. $\hat{f}_2(T_{exp},\ P_{exp},\ x_{2,exp})$ is the fugacity of the heavy component (2) in the fluid phase evaluated, with the model, at T_{exp}, P_{exp}, and $x_{2,exp}$. $f_2^S(T_{exp},\ P_{exp})$ is the fugacity of the pure heavy component (2) in solid state evaluated, with the model, at T_{exp} and P_{exp}. The summation is over the *NP* solid–fluid equilibrium points selected as indicated in the footnotes of Table 2. Actually the solid–liquid–vapor (SLV) equilibrium information given in Table 2 was not included in the objective function due to the lack of experimental information on the composition of the fluid phases at SLV equilibrium. Notwithstanding, in the selection of experimental data points, to be used in the objective function, we considered that the resulting set of parameters should be able not only to represent the experimental solid–fluid equilibrium data but also the temperature-pressure coordinates of the (in a way, actually unique) experimental solid–fluid–fluid equilibrium point found in this work at 303.15 K (see Section 4). During the optimizations, we did find some sets of parameters that were able to properly reproduce the SF data but not the SFF point. This is not a trivial matter: the location of the SFF equilibrium loci given by the model has a great influence on the predicted phase behavior of the mixture over a wide range of conditions.

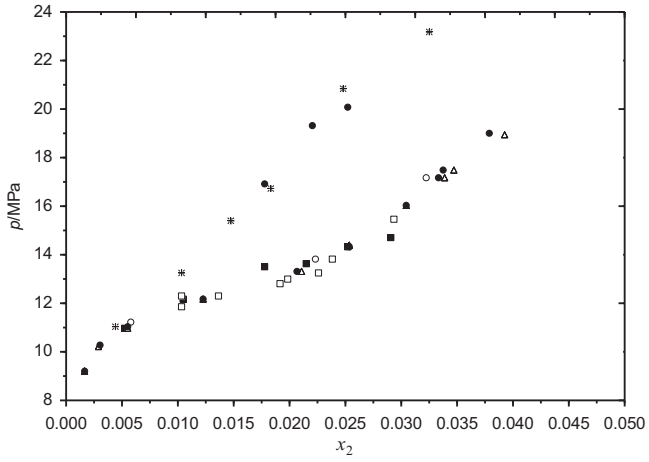

Fig. 3. Experimental pressure-composition diagrams for the systems CO_2(1) + naphthalene(2) and CO_2(1) + biphenyl(2) under solid–fluid equilibrium conditions. System CO_2(1) + naphthalene(2) at 328 K: ■: Present apparatus and experimental procedure [10]; △: McHugh and Paulaitis [38]; ○: Chang and Morrell [39]; □: Zúniga-Moreno et al. [37]). System CO_2 (1) + biphenyl(2) at 328 K: ●: Present apparatus and experimental procedure [10]; ✱: McHugh and Paulaitis [38]. The variable x_2 is the mole fraction of the heavy component in the fluid phase.

The final values used in this work for the binary interaction parameters (k_{12} and l_{12}) are given in Table 4, while the final value for Δv^{S-L} is given in Table 5, which also reports other pure MPgAc characteristic constants. They are needed for evaluating the variable *U* of Eq. (1′) of Appendix A. The meaning of the constants is explained in Appendix A and in Table 5. For more details on possible ways of parameterizing the model used in this work see Refs. [29,21].

4. Results

4.1. Experimental results

The experimental apparatus and methodology used in this work have been thoroughly tested in previous works corresponding to the study of solid–fluid phase equilibria. See, e.g., Refs. [10,21–26,34,35]. Favareto et al. [10] have shown that the present aparatus and experimental procedure is able to reproduce the experimental solubility data of CO_2 (1) + naphthalene (2) and CO_2 (1) + biphenyl (2) available in the literature [36–39]. This is shown in Fig. 3.

Table 2 presents the phase transition data measured in this work for the system CO_2 (1) + MPgAc (2) at temperatures from 303.15 K to 343.15 K and at global CO_2 mole fraction (x_1) values from 0.99991 to 0.99996 [i.e., at global MPgAc mole fraction (x_2) values from 4×10^{-5} to 9×10^{-5}]. The results are presented in terms of temperature, composition, transition pressure and type of phase transition. σ is the standard deviation of replicate measurements of the transition pressure. The pressure values reported in Table 2 have an estimated uncertainty in the order of 1%. Table 2 shows the occurrence of SF (solid + fluid) and SFF (solid + fluid + fluid) equilibria. In the case of SF transitions the reported composition is regarded as that of the equilibrium fluid phase, since such fluid phase is at equilibrium with a solid phase of negligible size (incipient phase). The measured SFF points correspond to solid–liquid–vapor (SLV) equilibria, where (in general) none of the phases has a composition equal to the SLV overall composition reported in Table 2. As shown in Table 2, we have experimentally found a SLV point for every isopleth. This has happened at 303.15 K in all cases. Table 2 shows that the pressure of the SLV point is practically independent from the isopleth composition and has a value of about 7.2 MPa. This is

Table 2
Experimental solid–fluid (SF) and solid–liquid–vapor (SLV) transition data for CO_2 (1) + medroxiprogesterone acetate (2) binary mixtures. (This work. BP: bubble point.).

T (K)	P (MPa)	σ (MPa)	Transition type	T (K)	P (MPa)	σ (MPa)	Transition type
$x_1 = 0.999910$, $x_2 = 0.000090$				$x_1 = 0.999946$, $x_2 = 0.000054$			
303.15	14.587	0.04	SF[a]	303.15	11.027	0.02	SF
313.15	16.803	0.02	SF	313.15	13.42	0.02	SF
323.15	18.647	0.04	SF	323.15	15.646	0.03	SF
333.15	20.247	0.01	SF	333.15	17.634	0.03	SF
343.15	21.774	0.01	SF	343.15	18.71	0.01	SF
303.15	7.163	0.02	SLV (BP)[b]	303.15	7.18	0.01	SLV (BP)[b]
$x_1 = 0.999926$, $x_2 = 0.000074$				$x_1 = 0.999960$, $x_2 = 0.000040$			
303.15	13.897	0.01	SF	303.15	9.284	0.03	SF[a]
313.15	15.63	0.04	SF	313.15	11.413	0.06	SF
323.15	17.7	0.04	SF	323.15	13.797	0.04	SF
333.15	19.267	0.03	SF	333.15	15.464	0.02	SF
343.15	20.44	0.04	SF	343.15	17.347	0.05	SF[a]
303.15	7.17	0.03	SLV (BP)[b]	303.15	7.17	0.03	SLV (BP)[b]
$x1 = 0.999936$, $x2 = 0.000064$							
303.15	12.713	0.01	SF				
313.15	14.847	0.06	SF				
323.15	16.69	0.01	SF				
333.15	18.374	0.02	SF				
343.15	19.337	0.03	SF				
303.15	7.13	0.02	SLV (BP)[b]				

[a] Solid–fluid experimental data considered for the fitting of the binary interaction parameters ($k12$, l_{12}) of the PR-EOS together with parameter Δv^{S-L} of Eq. (1′) in Appendix A (see Tables 4 and 5).
[b] SLV experimental data also considered in the parameter fitting.

consistent with the Phase Rule, which establishes that a three-phase equilibrium of a binary system has a single degree of freedom, i.e., once the temperature is set at a value of 303.15 K, then, the value for the pressure at SLV equilibrium becomes defined, regardless the overall concentration of MPgAc in the heterogeneous system. We have taken the SLV equilibrium pressure at 303.15 K as the average value of the SLV pressures reported in Table 2. Experimentally, we found SLV points as follows: first, we looked for a solid–fluid transition as already described in Section 2.2. Next, under solid–fluid conditions, we reduced the pressure further until we observed the appearance of a third (fluid) phase.

Notice that the experimental pressure and temperature conditions (303.15 K and 7.2 MPa) of the SLV point found in this work are very close to the P and T conditions of the pure carbon dioxide critical point (304.21 K and 7.383 MPa, see Table 3). Then, it is likely that the SLV curve, to which the SLV point here measured belongs, ends at a critical end point located very close to the critical point of carbon dioxide. Such behavior could correspond to a type F [29] behavior, in which case the measured SLV point would belong to the low-temperature SLV curve, i.e., not to the high-temperature SLV curve that would emanate from the pure MPgAc triple point, if the behavior were of type F. This is further discussed in Section 4.2 of the present work.

Fig. 4 presents the experimental solid–fluid transition pressure of system CO_2 (1) + MPgAc (2) as a function of temperature for a number of isopleths. The data are those of Table 2. The empty squares are SLV points with varying overall composition, but all having the same temperature and practically the same pressure. Consider for instance the isopleth at MPgAc mole fraction $x_2 = 9.0 \times 10^{-5}$ (full squares). The (not shown) continuous line that connects all the full squares in Fig. 4, sets the boundary between the single phase region, which lies above the line, and the heterogeneous region, located below the line, where two phases (fluid + solid) coexist (at least at conditions close enough to those of the line). Our experimental data (Fig. 4) behave as follows: (a) at constant MPgAc solubility, an increase in temperature implies an increase in the SF equilibrium pressure; (b) at constant temperature, an increase in pressure gives a decrease in solubility; (c) at constant pressure, an increase in temperature gives an increase in solubility. In other words, within the ranges of conditions of our experimental data, pressure and temperature have opposite effects on the MPgAc solubility in CO_2.

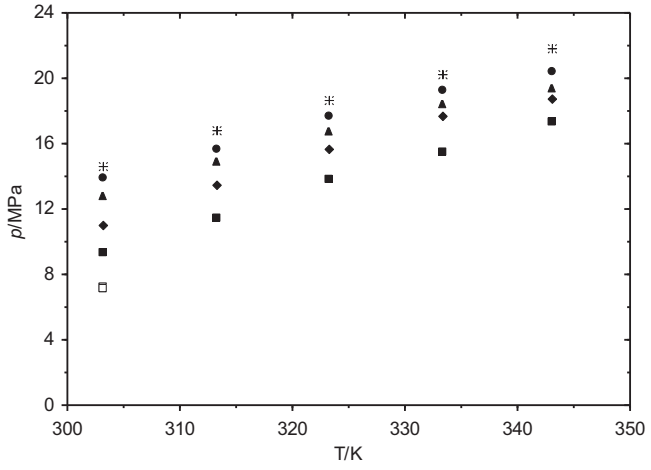

Fig. 4. Experimental phase equilibrium data for CO_2 (1) + MPgAc (2) mixtures obtained in this work at the following global MPgAc mole fractions: $x_2 = 9.0 \times 10^{-5}$ (■, SFE; □, SFFE); 7.4×10^{-5}(♦, SFE; □, SFFE); 6.4×10^{-5}(▲, SFE; □, SVLE); 5.4×10^{-5}(●, SFE; □, SFFE) and 4.0×10^{-5} (✳, SFE; □, SFFE).

4.2. Comparison with SFE data from the literature

Fig. 5 presents experimental solubilities of MPgAc in CO_2 as a function of pressure at varying temperatures. The data are from this work and from Alessi et al. [11]. The agreement is good at 313 K. However, the data from Alessi et al. [11] at 333 K are closer to our data at 323.15 K than to our data at 333.15 K, except in the lowest solubility range, where the agreement is better. Within the pressure ranges of the experimental data, the fluid phase is always a quite dense fluid. The pressure of dense fluids is quite sensitive to small changes in temperature. The abscissa of Fig. 5, i.e., the pressure, could be replaced by a variable expected to have, in relative terms, a limited sensitivity to pressure. The compressibility factor of the pure solvent (CO_2) at the experimental temperature and pressure

Table 3
Properties of pure compounds.

Compound	T_b (K)	T_{crit} (K)	P_{crit} (MPa)	υ_{crit} (cm^3 mol^{-1})	ω
CO_2		304.21[a]	7.383[a]		0.223621[a]
Medroxiprogesterone acetate	660.0[b]	851.0[b]	1.316[b]	1144.64[b]	0.851112[b]

T_b = boiling temperature. T_{crit} = critical temperature. P_{crit} = critical pressure. υ_{crit} = critical volume. ω = acentric factor.
[a] From DIPPR database [32].
[b] Estimated values for the properties of pure medroxiprogesterone acetate using Constantinou and Gani group contribution method [33].

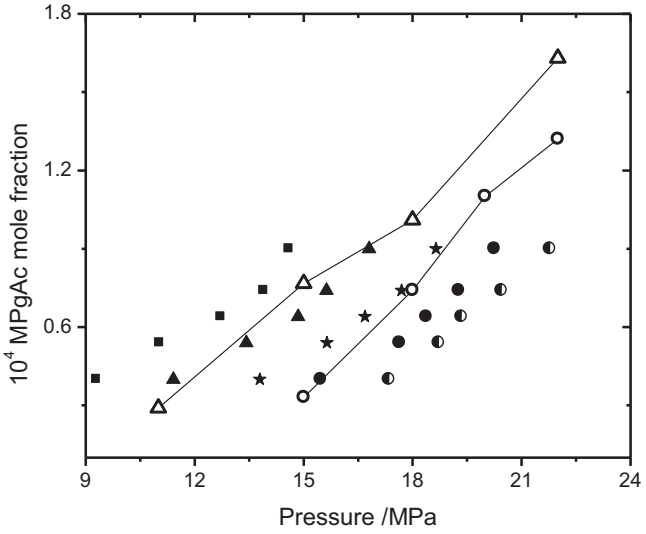

Fig. 5. Experimental solubility of MPgAc in CO_2 as a function of pressure at varying temperatures: ■: 303.15 K, ▲: 313.15 K, ★: 323.15 K, ●: 333.15 K, ◐: 343.15 K (this work, synthetic static method). -△- 313 K, -○- 333 K (Alessi et al. [11], analytical dynamic method).

seems to be a good choice, since the pressure appears both (directly) in the numerator and (indirectly through density, which increases with pressure at constant temperature) in the denominator. In this sense, Fig. 6 shows the experimental solubility of MPgAc in CO_2 as a function of the pure CO_2 compressibility factor, at varying temperatures. Now we see that the degree of agreement at 333 K is greater than in Fig. 5, and that at 313 K the agreement seems to remain as good as in Fig. 5. Fig. 7 is analogous to Fig. 6. Fig. 7 compares our experimental data with those of Asghari-Khiavi et al. [12]. The disagreement appears to be more important than in Fig. 6. A difficulty in performing this comparison is that the temperature values of the data of Ref. [12] are not the same than those of our data. In conclusion, our data seem to have a higher level of agreement with the data by Alessi et al. [11] than with the data by Asghari-Khiavi et al. [12]. Measurements independently performed in the future by other laboratories for CO_2 + MPgAc would be most welcome, to obtain more definitive conclusions on the solubility of MPgAc in CO_2.

4.3. Modeling results

The calculated average percent absolute-value relative deviation (%AARD), corresponding to the quantitative comparison between the model and the experimental solid–fluid equilibrium data of Table 2 is 4.5%. The %AARD was calculated as follows:

$$\%AARD = \frac{100}{ND}\sum_{ND}\left|\frac{P_{exp} - P_{calc}}{P_{exp}}\right| \quad (2)$$

In Eq. (2), *ND* is the total number of experimental solid–fluid data points in Table 2, P_{exp} is the experimental pressure value. P_{calc} is the solid–fluid equilibrium pressure predicted by the model at the experimental temperature (T_{exp}) and experimental fluid

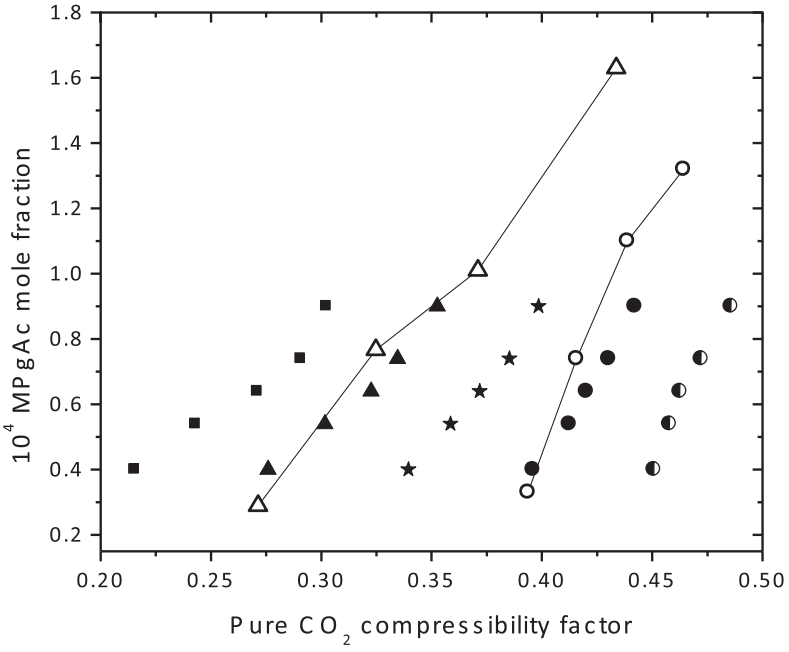

Fig. 6. Experimental solubility of MPgAc in CO_2 as a function of pure CO_2 compressibility factor at varying temperatures. ■: 303.15 K, ▲: 313.15 K, ★: 323.15 K, ●: 333.15 K, ◐: 343.15 K (this work, synthetic static method). -△- 313 K, -○- 333 K (Alessi et al. [11], analytical dynamic method). The compressibility factor was obtained at the experimental temperature and pressure using the NIST WebBook [40].

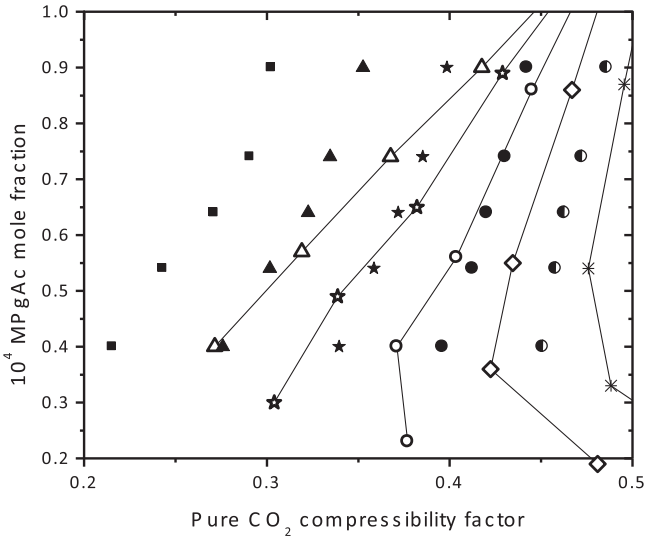

Fig. 7. Experimental solubility of MPgAc in CO_2 as a function of pure CO_2 compressibility factor at varying temperatures. ■: 303.15 K, ▲: 313.15 K, ★: 323.15 K, ●: 333.15 K, ◐: 343.15 K (this work, synthetic static method). -△- 308 K, -☆- 318 K, -◯- 328 K, -◇- 338 K, -✳- 348 K (Asghari-Khiavi et al. [12], analytical static method). The compressibility factor was obtained at the experimental temperature and pressure using the NIST WebBook [40].

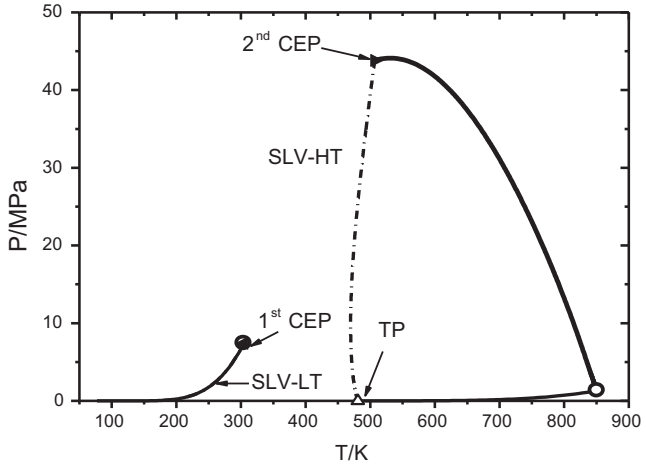

Fig. 8. Pressure (P)-temperature (T) projection of calculated univariant lines for the binary system CO_2 (1) + medroxiprogesterone acetate (2). —: critical loci, –– pure compound saturation curve (vapor–liquid), -·-·- three-phase curves: solid–liquid–vapor (SLV-LT and SLV-HT), empty circle: pure compound critical point, empty triangle: pure compound triple point (TP), ◄: first critical end point (1st CEP), ►: second critical end point (2nd CEP). Model: see Appendix A. Model parameters from Tables 4 and 5. The predicted phase behavior corresponds to TYPE F [29].

Table 4
Binary interaction parameters obtained in this work for the PR-EoS [28].

System	k_{12} (attractive)	l_{12} (repulsive)
Carbon dioxide (1) + medroxiprogesterone acetate (2)	2.687×10^{-3}	0.1493

phase composition ($x_{2,exp}$) (Table 2), using the parameter values of Tables 4 and 5.

The model predicts, for the system CO_2 (1) + MPgAc (2), a phase behavior of type F [29] at the parameters values of Tables 3–5 (see Fig. 8). The type F behavior [29] presents a critical line which stems from the critical point of the heavy compound (i.e., medroxiprogesterone acetate in this case [empty circle at high temperature in Fig. 8]) and ends at a second critical end point (2nd CEP). From this CEP, a solid–liquid–vapor locus (SLV-HT) starts and ends at lower pressure, at the triple point (TP) of the heavy compound. At a CEP, of the type relevant to this work, a critical fluid phase is in equilibrium with the pure heavy compound in solid state. Moreover, another (very short) critical line originates at the critical point of the light compound (i.e., CO_2) and ends at a first critical end point (1st CEP), from which a solid–fluid–fluid locus stems and extends to low temperatures (SLV-LT). The scale of Fig. 8 is such that the pure CO_2 vapor–liquid coexistence curve appears to coincide with the SLV-LT curve. This is also the case for the pure CO_2 critical point and the 1st CEP, which are indeed very close. The model, with the parameters values of Tables 3–5, predicts the following temperature, pressure, and composition values for the 1st CEP: 304.2 K, 7.38 MPa and $x_2 = 2.29 \times 10^{-7}$; and for the 2nd CEP: 506.8 K, 43.8 MPa and $x_2 = 0.05008$. Consistently, the calculated temperature and pressure of the 1st CEP are slightly higher than the temperature and pressure of the SLV equilibrium point measured in this work. A full schematic pressure–temperature projection of the type F behavior is shown in Ref. [29].

In Fig. 9, we present the pressure-composition projection of the SFF loci of Fig. 8. The solid phase is always pure medroxiprogesterone acetate for either SFF locus. At a CEP the two fluid phases at SFF equilibrium become identical. In Fig. 9 it is possible to read, at a set pressure, the mole fraction of MPgAc in each of the two fluid phases of a solid–fluid–fluid equilibrium point. At high enough pressure, only one SFF locus exists. At low pressure, both SFF loci exist. The temperature corresponding to a set SFF equilibrium

Table 5
Medroxiprogesterone acetate constants for Eq. (1′) in Appendix A.

T_{tp} (K)[a]	481
P_{tp} (MPa)[b]	4.3369×10^{-4}
Δv^{S-L} (m^3/K mol)	−0.42551
C_1 (MPa)	−150.0
C_2 (MPa)	0
C_3 (MPa)	0

[a] Experimentally obtained in this work (see Table 1).
[b] P_{tp}: pure compound vapor–liquid equilibrium pressure calculated at the triple point temperature T_{tp} using the PR-EOS [28].

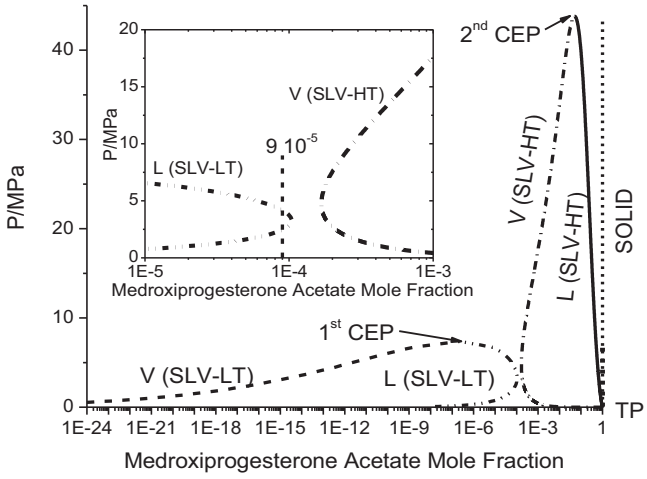

Fig. 9. Pressure-composition projection of calculated solid–liquid–vapor (SLV) equilibrium curves for the system CO_2 (1) + medroxiprogesterone acetate (2). SLV-HT is the SLV line that starts at the triple point (TP) of the pure MPgAc and ends at the second critical end point (2nd CEP); and SLV-LT is the SLV locus that originates at the first critical end point (1st CEP) and extends toward low temperatures and pressures. V: vapor phase. L: liquid phase. Model: see Appendix A. Model parameters from Tables 4 and 5.

pressure is read in Fig. 8. Fig. 9 is useful to quickly establish how many SFF equilibrium points will appear in the calculated phase envelope of a given isopleth. For instance, the isopleth corresponding to 9×10^{-5} MPgAc mole fraction (see inset in Fig. 9), must have two SFF equilibrium points.

In Fig. 10(a) we present an isopleth for the CO_2 (1) + medroxiprogesterone acetate (2) mixture, calculated using the PR-EOS and Eq. (1′) from Appendix A. The isopleth corresponds to 9×10^{-5} MPgAc fluid phase mole fraction, i.e., to the highest MPgAc concentration in Table 2. The phase envelope, presents solid–fluid (SF) and fluid–fluid (FF) transition lines. The relevant segments of the calculated solid-liquid–vapor lines are included in the heterogeneous region of the isopleth.

At high pressure and low temperature, we observe in Fig. 10(a) a SF transition segment that extends to low pressure and intersects a liquid–vapor equilibrium line (FF, bubble point line) at about 2.46 MPa. This intersection point (full circle) is a three-phase (solid–liquid–vapor) equilibrium point at 9×10^{-5} MPgAc mole fraction for one of the fluid phases (see inset in Fig. 9). The liquid–vapor (LV, FF) segment (bubble line) that originates at such three-phase point extends up to a maximum pressure of 4.23 MPa where it intersects, at a second three-phase point, another SF transition segment. This second SF segment goes through a local maximum in pressure, then through a local maximum in temperature, and it finally continues toward low pressures. In Fig. 10(a) the SFF line, i.e., the SLV-LT locus, sets boundaries between sub-regions within the heterogeneous region. Thus, this SLV line completes the portrayal of the phase behavior inside the heterogeneous region of the isopleth.

The SF experimental data [empty squares in Fig. 10(a)] agree well with the model (dash-dot line). Similarly, the only solid–liquid–vapor equilibrium point measured in this work [triangle in Fig. 10(a)] agrees well with the calculated SLV equilibrium line (SLV-LT line) that ends at the 1st CEP.

Fig. 10(b) is a zoom of Fig. 10(a). A mixture at the conditions of point A in Fig. 10(b) has a SF behavior (i.e., solid–vapor). If we cool the mixture, at constant pressure, we will observe a three-phase SFF system (SLV in this case) at point B. If we continue cooling the mixture, we will observe a SF (solid–liquid) behavior at point C, but the nature of the fluid phase is liquid. This SL behavior will be observed up to point D, and by further lowering the temperature we will have an homogeneous system (single liquid phase), e.g., at point E. Finally, at point F, a SF behavior will appear again, and will remain at lower temperatures.

At the scale of Fig. 10(b) it is not possible to see the SFF segment that is located below the FF line, between the two full circles. Such SFF also contributes to the characterization of the heterogeneous region.

Fig. 10(a) includes the whole SLV-LT locus, because the composition of the isopleth (9×10^{-5} MPgAc mole fraction) is in between the extreme compositions of the phases of the SLV-LT equilibrium line everywhere on such line (see the inset in Fig. 9). Moreover, no segments of the SLV-HT locus were included in Fig. 10(a) and (b), because the composition of the isopleth (9×10^{-5} MPgAc mole fraction) is never in between the vapor phase composition (lightest phase) and the solid phase composition (pure MPgAc, heaviest phase), regardless the pressure condition. Otherwise, all phases of the SLV-HT line have a MPgAc concentration always greater than 9×10^{-5} MPgAc mole fraction (see Fig. 9 and its inset).

It is important to stress that at a pressure about 12.5 MPa the two SF segments of Fig. 10(a) and (b) almost meet each other. However, they do not do it, as it is more clearly shown in Fig. 10(b).

Notice that the present model, used with the parameters of Tables 3–5, captures the qualitative behavior observed experimentally in the laboratory during the measurement process, in particular in the one performed at low enough temperature. This can be clearly seen from Fig. 10(b). For example, at the temperature (303.15 K) and pressure conditions of point 1 in Fig. 10(b), the model gives a homogeneous fluid state (liquid). If we decrease the pressure at constant temperature, i.e., at 303.15 K, from point 1 to point 3, we reach a heterogeneous solid–fluid condition (at point 3). At such temperature, the limit between the homogeneous and heterogeneous states is located at point 2, where the fluid (liquid) phase is saturated in MPgAc (i.e., the liquid is at equilibrium with a pure MPgAc incipient solid phase). Then, if we continue decreasing the pressure, we will reach a three-phase equilibrium condition at point 4 (SLV in this case). A further decrease in pressure results again in a SF equilibrium condition (point 5). At point 5 the fluid phase is a vapor phase. It is clear that in the transition from point 1 to point 3 in Fig. 10(b) a solid phase appears upon a pressure reduction. Thus, we recognize the process that takes the binary system from point 1 to point 3 as retrograde solidification at constant temperature (RSCT). The experimental data indicate the existence of RSCT, and the model properly captures such behavior, as seen in Fig. 10(a)–(f).

From Fig. 10(a), we notice that the model [PR-EoS and Eq. (1′) of Appendix A] predicts that at any temperature lower than about 260.7 K, i.e., lower than the lowest temperature at which a SF line and a FF line meet), it would not be possible to observe a dense homogeneous fluid system, even at very high pressure conditions [at least up to 25.0 MPa, which is the maximum pressure shown in Fig. 10(a)]. In other words, at a temperature lower than 260.7 K, it would not be possible, starting from a dense homogeneous system, to detect a phase transition by decreasing pressure, because such dense homogeneous system simply does not exist.

In Fig. 10(a), and according to the model, at about 20.0 MPa and 475 K, the system is a homogenous fluid (made of only one phase). Then, by decreasing the temperature while keeping the pressure constant at 20.0 MPa, a solid phase, pure MPgAc, appears when the solid–fluid line is crossed for the first time. The system presents two phases (SF system), and the fluid phase has the composition of the isopleth. If we continue decreasing the temperature, the relative quantity of the solid phase augments and then, it diminishes [retrograde melting at constant pressure (RMCP)]. Finally the solid phase disappears when the SF boundary is crossed again, i.e., when an homogeneous system condition is again reached. A further decrease in temperature makes the solid phase reappear (normal solidification) when the second SF boundary is crossed. This solid–fluid coexistence remains present even at very low temperatures.

Fig. 10(c)–(f) correspond to CO_2 + MPgAc isopleths in the range from 7.4×10^{-5} to 4×10^{-5} MPgAc mole fraction. They qualitatively behave as the isopleth of Fig. 10(a), i.e., they all have: (A) a FF segment, a couple of SF segments and two SFF points in the isopleth phase envelope, and (B) the full SLV-LT line in the isopleth heterogeneous region. Fig. 10(c)–(f) shows that the separation between the two calculated SF segments increases with the decrease in the MPgAc mole fraction. This is also the case for the temperature range of existence of the calculated FF lines. We again find a good level of agreement between model and experiment when we observe Fig. 10(c)–(f).

In, e.g., Fig. 10(f), the calculation results obtained with the model suggest that there is a pressure range within which it is possible to reach, at constant pressure, solid–fluid transitions from an initial homogeneous fluid state, either by increasing the temperature (retrograde behavior) or by decreasing the temperature (normal behavior), as long as such initial homogeneous fluid state corresponds to a point located in between the two SF segments. Of both phenomena, the retrograde behavior is confirmed by our experimental data (squares) in, e.g., Fig. 10(f). For example, considering an initial SF condition at 350 K and 15.0 MPa, a decrease in temperature takes the system to a single phase region after the SF segment is

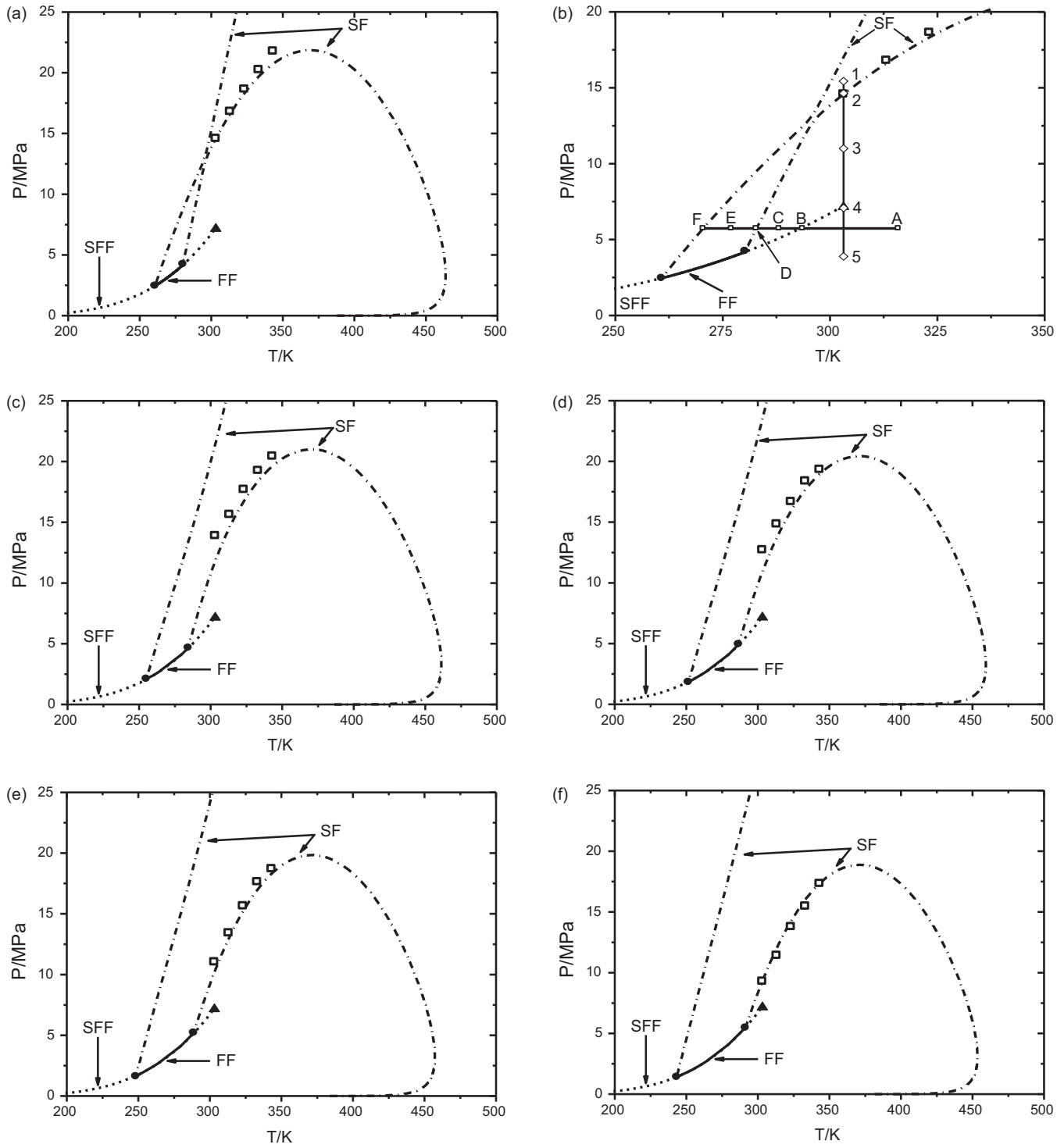

Fig. 10. Calculated isopleths for the CO_2 (1) + medroxiprogesterone acetate (2) mixture. Fluid phase medroxiprogesterone acetate mole fraction values: Fig. 10 (a): 9×10^{-5}, Fig. 10 (b): 9×10^{-5} [zoom of Fig. 10(a)], Fig. 10(c): 7.4×10^{-5}, Fig. 10(d): 6.4×10^{-5}, Fig. 10(e): 5.4×10^{-5}, Fig. 10(f): 4.0×10^{-5}. □: experimental solid–fluid equilibrium data (this work, Table 2); ▲: experimental solid–liquid–vapor equilibrium datum (this work, Table 2). Phase equilibria calculated using the PR-EoS and Eq. (1′) of Appendix A: ■■■■ solid–fluid, ▬▬ bubble line (fluid–fluid), ■■■■ and ● solid–fluid–fluid points. A portion of the SFF line connects the two full circles: at the scale of the figure such portion appears to be coincident with the FF line, but it is actually located below it. Model parameters from Tables 4 and 5.

crossed (retrograde melting at constant pressure, RMCP). A further decrease in temperature takes the system again to a SF condition at low enough temperature (normal solidification at constant pressure) after the lower temperature SF segment is intersected. This complex behavior is due to the highly curved SF line that exists at intermediate (and high) temperatures. It should be clear that for a system showing RMCP it is possible to melt a solid phase by decreasing the temperature. The phenomenon of retrograde melting at constant pressure could be attributed to the decrease of the solvent (CO_2) density [and the corresponding behavior of its dielectric constant (reduction of solvent power)], when temperature is raised under conditions relatively close to the critical conditions of the solvent (carbon dioxide) [21]. The solid–fluid segments predicted by the model for this isopleth conform to the common sense

expectation that at low enough temperature a solid phase must be present in the system. This must happen even in the case of existence of RMCP.

5. Remarks and conclusions

In this work we provide, for the system CO_2 (1) + MPgAc (2), new experimental data on solid–fluid (SF) and solid–fluid–fluid (SFF) transitions for five isopleths in the low MPgAc concentration range (medroxiprogesterone acetate mole fractions: 9×10^{-5}, 7.4×10^{-5}, 6.4×10^{-5}, 5.4×10^{-5}, and 4×10^{-5}). Our data seem to have a higher level of agreement with the data by Alessi et al. [11] than with the data by Asghari-Khiavi et al. [12]. The experimental methods in Refs. [11,12] are analytical, while the one used in this work is synthetic. Our experimental data show that pressure and temperature have opposite effects on the MPgAc solubility in CO_2, within the experimental ranges of conditions covered in this work.

The phase behavior experimentally observed in this work (solid–fluid and solid–fluid–fluid transitions) is properly captured by a model built by combining the Peng–Robinson equation of state (PR-EoS, with classical combining and mixing rules) with an equation that describes the fugacity of pure compounds in solid state, i.e., Eq. (1′) of Appendix A.

For all isopleths studied here, the experimental data show the occurrence of retrograde melting at constant pressure (RMCP), for medroxiprogesterone acetate in CO_2, which means that it is possible to melt the solid phase by decreasing the temperature. The RMCP is also described by our model. The experimental data also present retrograde solidification at constant temperature (RSCT), which the model also captures.

The numerical continuation methods used in the calculations were essential to track the highly non-linear solid–fluid equilibrium curves computed with the model [29].

The calculated isopleths, an the calculated SFF loci (Figs. 8 and 9), have temperature ranges wider than the temperature range studied experimentally. In spite of the potentially important errors that, from the quantitative point of view, such extrapolations may carry, the calculation results obtained in the present work, over wide ranges of conditions, are useful to enhance our understanding of the possible qualitative, highly non-ideal, behavior of the present and related systems.

Acknowledgments

We are grateful to Mr Pablo Salazar, for useful comments and, for their financial support, to the following institutions: Capes/Brazil, Fundação Araucária (Brazil), FAPESP (Brazil), CNPq (Brazil), Consejo Nacional de Investigaciones Científicas y Técnicas de la República Argentina (CONICET), Universidad Nacional del Sur (U.N.S., Arg.), and Agencia Nacional de Promoción Científica y Tecnológica (ANPCyT, Arg.). M. S. Z. was a CAPES/BRASIL Grantee at State University of Maringá during part of year 2013.

Appendix A. Thermodynamic model

The model used in this work for describing phase equilibria involving fluid and solid phases is the same than the model used in previous works [21,27,29]. To describe the fluid state of a binary mixture of a light component (labeled "1") and a heavy component (labeled "2"), we use a pressure-explicit equation of state (EOS), i.e., a relationship between the absolute pressure (P), the absolute temperature (T), the mixture molar volume (υ) and the mixture composition z_2, where z_2 is the mole fraction of component "2".

We represent such relationship as $P = h_{PVT}(T, z_2, \upsilon)$, where the form of function h_{PVT} corresponds to the adopted EOS, e.g., to the Peng–Robinson (PR) [28] EOS, i.e., the EOS that we used in this work. The h_{PVT} function, imposes the expression for the fugacity of component "i" in the fluid mixture ($\hat{f}_i$). Thus, $\hat{f}_i$ depends on the same variables than function h_{PVT}, i.e., $\hat{f}_i = \hat{f}_i(T, z_2, \upsilon)$. Indeed, this last functional relationship also corresponds in this work to the PR-EOS [28].

Due to the high asymmetry of the binary system that we consider in this work, we assume that a given solid phase is made of only the pure heavy component (component "2", i.e., medroxiprogesterone acetate in this work). Thus, for performing equilibrium calculations, we need an equation relating the fugacity of the pure component "2" in solid state to the absolute pressure (P) and to the absolute temperature (T) of the system. We define, mathematically, the fugacity of the pure heavy component "2" in solid state at T and P, i.e., $f_2^S(T, P, \upsilon)$ (where υ_o actually depends on T and P) as follows:

$$f_2^S(T, P, \upsilon_o) = \hat{f}_2(T, 1, \upsilon_o) \exp(U) \tag{1′}$$

In Eq. (1′), υ_o is the molar volume of the pure heavy component (component "2"), in (subcooled hypothetical) liquid state, at T and P. Such pure liquid has a fugacity $\hat{f}_2(T, 1, \upsilon_o)$ [first factor within the right hand side of Eq. (1′)]. Notice that expression $\hat{f}_2(T, 1, \upsilon_o)$ simply states that the function $\hat{f}_i = \hat{f}_i(T, z_2, \upsilon)$, with subscript "$i$" set equal to "2", is evaluated at $z_2 = 1$ and at $\upsilon = \upsilon_o$, i.e., that the computed fugacity corresponds to a liquid made of the pure heavy compound, having such pure liquid a molar volume equal to υ_o. Both, υ_o and $\hat{f}_2(T, 1, \upsilon_o)$ are given in this work by the PR-EOS [28].

The exponential factor in Eq. (1′) relates [through Eq. (1′)] the hypothetical liquid state with the solid state for a pure substance at given temperature and pressure. The variable U, which depends on T and P, is defined as follows:

$$U = \frac{\Delta\upsilon^{S-L}}{RT_{tp}} \left[C_1 \left(1 - \frac{T_{tp}}{T}\right) + C_2 \left(\frac{T_{tp}}{T} - 1 + \ln\left(\frac{T_{tp}}{T}\right)\right) + C_3 \left(\frac{T}{2T_{tp}} - 1 + \frac{T_{tp}}{2T}\right) + \frac{T_{tp}}{T}(P - P_{tp}) \right] \tag{2′}$$

In Eq. (2′), the constants T_{tp}, P_{tp}, $\Delta\upsilon^{S-L}$, C_1, C_2, *and* C_3 (see Table 5 in the main text) correspond to the pure heavy component (component "2"). $\Delta\upsilon^{S-L}$ is the solid-liquid molar volume difference ($\upsilon_{solid} - \upsilon_{liquid}$). The constants C_1, C_2 and C_3 characterize the pure heavy component solid–liquid equilibrium curve (P versus T melting curve, [27]). Notice that the variable U is equal to zero at every point of the pure heavy component melting curve. The condition $U = 0$ set in Eq. (2′) makes possible to obtain the melting pressure as a function of temperture T and of the parameters T_{tp}, P_{tp}, C_1, C_2 and C_3. More details on the physical meaning of constants C_1, C_2 and C_3 are given in Appendix B of Ref. [29]. R is the universal gas constant.

For computing $f_2^S(T, P, \upsilon_o)$ at set T and P, we would first calculate υ_o from the adopted EOS [$P - h_{PVT}(T, 1, \upsilon_o) = 0$], next we would compute $\hat{f}_2(T, 1, \upsilon_o)$, then U from Eq. (2′), and, finally, plug the results into de right hand side of Eq. (1′), to obtain the value of $f_2^S(T, P, \upsilon_o)$. We stress that the phase type for $f_2^S(T, P, \upsilon_o)$ is "solid" while the phase type for $\hat{f}_2(T, 1, \upsilon_o)$ is "liquid", and that both fugacities correspond to the same T and P values.

The variable υ_o, i.e., a property of a pure liquid, appears as an argument for the fugacity of the pure solid [on the left hand side of Eq. (1′)] because the fugacity of the pure solid is partially computed from the fugacity of the pure liquid, i.e., from a liquid-state reference fugacity, being the temperature and pressure for such reference fugacity the same than the temperature and pressure of the solid.

The calculation of a binary phase equilibrium point requires solving the isofugacity condition for component "1" in all fluid phases and for component "2" in all fluid phases and in the solid

phase (if present), after imposing the constraint of uniform pressure and uniform temperature throughout the heterogeneous system.

More details on the model used here were given by Rodriguez-Reartes et al. [29].

References

[1] V.M. Portela, A.M. Farias, J.C.F. Moraes, P.B.D. Gonçalves, A.P.M. Veiga, J.F. Oliveira, Effect of medroxy-progesterone acetate on follicular growth and endometrial cycloxygenase-2 (COX-2) expression during the bovine estrous cycle, Pesquisa Veterinária Brasileira 30 (2010) 581–585.

[2] L.F.K. Borges, R. Ferreira, L.C. Siqueira, R.C. Bohrer, J.W. Borstmann, J.F.C.d. Oliveira, P.B.D. Gonçalves, Artificial insemination system without estrous observation in suckled beef cows, Ciência Rural 39 (2009) 496–501.

[3] L.C. Siqueira, J.F.C. Oliveira, R.D.S. Loguércio, H.K. Löf, P.B.D. Gonçalves, Sistemas de inseminação artificial em dois dias com observação de estro ou em tempo fixo para vacas de corte amamentando, Ciência Rural 38 (2008) 411–415.

[4] M. Meneghetti, J.L.M. Vasconcelos, Mês de parição, condição corporal e resposta ao protocolo de inseminação artificial em tempo fixo em vacas de corte primíparas, Arquivo Brasileiro de Medicina Veterinária e Zootecnia 60 (2008) 786–793.

[5] D. Burn, B. Ellis, V. Petrow, I.A. Stuart-Webb, D.M. Williamson, 809. Modified steroid hormones. Part IV. 6-Methylpregnane derivatives, J. Chem. Soc. (Resumed) (1957) 4092–4098.

[6] A.F. Rathke, D. Poester, J.F. Lorenzatto, V.B. Schimidt, L.D. Helter, Contracepção hormonal contendo apenas progesterona, Adolesc. Latinoam. 2 (2001) 90–96.

[7] J.R. Campos, V.H. Melo, Depot medroxyprogesterone acetate as an injectable contraceptive for adolescents, Rev. Bras. Ginecol. Obstet. 23 (2001) 181–186.

[8] The United States Pharmacopeia: The National Formulary–25th ed. United States Pharmacopeial Convention, Rockville, 2002.

[9] British Pharmacopeia, Her Majesty's Stationery Office, London, 1980.

[10] R. Favareto, J.R.D. Pereira, C.C. Santana, E.H. Madureira, V.F. Cabral, F.W. Tavares, L. Cardozo-Filho, High-pressure phase diagram of the drug mitotane in compressed and/or supercritical CO_2, J. Chem. Thermodyn. 42 (2010) 286–290.

[11] P. Alessi, A. Cortesi, I. Kikic, N.R. Foster, S.J. Macnaughton, I. Colombo, Particle production of steroid drugs using supercritical fluid processing, Ind. Eng. Chem. Res. 35 (1996) 4718–4726.

[12] M. Asghari-Khiavi, Y. Yamini, M.A. Farajzadeh, Solubilities of two steroid drugs and their mixtures in supercritical carbon dioxide, J. Supercrit. Fluids 30 (2004) 111–117.

[13] C.-S. Su, Y.-M. Chen, Y.-P. Chen, Correlation of solid solubilities for phenolic compounds and steroids in supercritical carbon dioxide using the solution model, J. Taiwan Inst. Chem. Eng. 42 (2011) 608–615.

[14] G.A. Sacha, W.J. Schmitt, S.L. Nail, Identification of critical process variables affecting particle size following precipitation using a supercritical fluid, Pharm. Dev. Technol. 11 (2006) 187–194.

[15] E. Kosal, C.H. Lee, G.D. Holder, Solubility of progesterone, testosterone, and cholesterol in supercritical fluids, J. Supercrit. Fluids 5 (1992) 169–179.

[16] C.-C. Huang, M. Tang, W.-H. Tao, Y.-P. Chen, Calculation of the solid solubilities in supercritical carbon dioxide using a modified mixing model, Fluid Phase Equilibr. 179 (2001) 67–84.

[17] T.F. Al-Azemi, L. Kondaveti, K.S. Bisht, Solvent less enantioelective ring-opening polymerization of substituted ε-caprolactones by enzymatic catalysis, Macromolecules 35 (2002) 3380–3386.

[18] S. Villarroya, K. Dudek, J. Zhou, D.J. Irvine, S.M. Howdle, Grafting polymers by enzymatic ring opening polymerisation-maximising the grafting efficiency, J. Mater. Chem. 18 (2008) 989–997.

[19] K.S. Oh, W. Bae, H. Kim, Dispersion polymerization of 2-hydroxyethyl methacrylate (HEMA) using siloxane-based surfactant in supercritical carbon dioxide and in compressed liquid dimethyl ether, Eur. Polym. J. 44 (2008) 415–425.

[20] B. Grignard, C. Jérôme, C. Calberg, R. Jérôme, C. Detrembleur, Atom transfer radical polymerization of MMA with a macromolecular ligand in a fluorinated solvent and in supercritical carbon dioxide, Eur. Polym. J. 44 (2008) 861–871.

[21] W.M. Giufrida, S.B. Rodriguez-Reartes, C.G. Alonso, M.S. Zabaloy, V.F. Cabral, F.W. Tavares, L. Cardozo-Filho, High-pressure experimental data of CO_2 + mitotane and CO_2 + ethanol + mitotane mixtures, J. Chem. Eng. Data 56 (2011) 4333–4341.

[22] H.R. Mazzer, J.C.O. Santos, V.F. Cabral, C. Dariva, M.H. Kunita, A.F. Rubira, M. Aznar, L. Cardozo-Filho, Phase behavior at high pressure of the ternary system: CO_2, ionic liquid and disperse dye, J. Thermodyn. 2012 (2012) 1–6.

[23] I. Prado, W. Giufrida, V. Alvarez, V. Cabral, S. Quispe-Condori, M.A. Saldaña, L. Cardozo-Filho, Phase equilibrium measurements of sacha inchi oil (*Plukenetia volubilis*) and CO_2 at high pressures, J. Am. Oil Chem. Soc. 88 (2011) 1263–1269.

[24] R. Favareto, P.H. Fregadolli, V.F. Cabral, O.A.C. Antunes, L. Cardozo-Filho, Phase equilibria of acrylonitrile and p-bromobenzaldehyde in carbon dioxide, J. Chem. Eng. Data 53 (2008) 1080–1084.

[25] L.S. Moura, R. Favareto, P.F. Leal, M.L. Corazza, L. Cardozo-Filho, M.A.A. Meireles, Phase equilibrium measurements for CO_2 + priprioca extract at high pressures, J. Supercrit. Fluids 48 (2009) 126–130.

[26] L.F. Pinto, P.M. Ndiaye, L.P. Ramos, M.L. Corazza, Phase equilibrium data of the system CO_2 + glycerol + methanol at high pressures, J. Supercrit. Fluids 59 (2011) 1–7.

[27] S.B. Rodriguez-Reartes, M. Cismondi, E. Franceschi, M.L. Corazza, J.V. Oliveira, M.S. Zabaloy, High-pressure phase equilibria of systems carbon dioxide + n-eicosane and propane + n-eicosane, J. Supercrit. Fluids 50 (2009) 193–202.

[28] D.-Y. Peng, D.B. Robinson, A new two-constant equation of state, Ind. Eng. Chem. Fund. 15 (1976) 59–64.

[29] S.B. Rodriguez-Reartes, M. Cismondi, M.S. Zabaloy, Computation of solid–fluid–fluid equilibria for binary asymmetric mixtures in wide ranges of conditions, J. Supercrit. Fluids 57 (2011) 9–24.

[30] M.L. Michelsen, Calculation of phase envelopes and critical points for multicomponent mixtures, Fluid Phase Equilibr. 4 (1980) 1–10.

[31] M.L. Michelsen, J.M. Mollerup, Thermodynamic Models: Fundamentals and Computational Aspects, 1st ed., Tie-Line Publications, Denmark, 2004.

[32] DIPPR 801, Evaluated Process Design Data, Public Release in, American Institute of Chemical Engineers, Design Institute for Physical Property Data, BYU-DIPPR, Thermophysical Properties Laboratory. Provo, Utah., 2003.

[33] R. Gani, L. Constantinou, Molecular structure based estimation of properties for process design, Fluid Phase Equilibr. 116 (1996) 75–86.

[34] J.C. dos Santos, H.R. Mazzer, G.D. Machado, J. Andreaus, V.F. Cabral, M.S. Zabaloy, L. Cardozo-Filho, High-pressure phase behaviour of the system (CO_2 + C.I. disperse orange 30 dye), J. Chem. Thermodyn. 48 (2012) 284–290.

[35] R. Favareto, V.F. Cabral, M.L. Corazza, L. Cardozo-Filho, Vapor-liquid and solid–fluid equilibrium for progesterone + CO_2, progesterone + propane, and progesterone + n-butane systems at elevated pressures, J. Supercrit. Fluids 45 (2008) 161–170.

[36] J.-W Chen, F. -N. Tsai, Solubilities of methoxybenzoic acid isomers in supercritical carbon dioxide, Fluid Phase Equilibr. 107 (1995) 189–200.

[37] A. Zúñiga-Moreno, L.A. Galicia-Luna, L.E. Camacho-Camacho, Measurements of solid solubilities and volumetric properties of naphthalene + carbon dioxide mixtures with a new assembly taking advantage of a vibrating tube densitometer, Fluid Phase Equilibr. 234 (2005) 151–163.

[38] M. McHugh, M.E. Paulaitis, Solid solubilities of naphthalene and biphenyl in supercritical carbon dioxide, J. Chem. Eng. Data 25 (1980) 326–329.

[39] H. Chang, D.G. Morrell, Solubilities of methoxy-1-tetralone and methyl nitrobenzoate isomers and their mixtures in supercritical carbon dioxide, J. Chem. Eng. Data 30 (1985) 74–78.

[40] E.W. Lemmon, M.O. McLinden, D.G. Friend, Thermophysical properties of fluid systems, in: P.J. Linstrom, W.G. Mallard (Eds.) NIST Chemistry WebBook, NIST Standard Reference Database Number 69, National Institute of Standards and Technology, Gaithersburg MD, 20899, http://webbook.nist.gov (retrieved July 5, 2012).